Incorporation of decellularized extracellular matrix in 3D-printed graphene-based scaffolds for treatment of volumetric muscle loss

Carlos Serna III[1], Rebecca Keate[2], Kristen Cotton[3], Matias Murillo[3], Yasmine Bouricha[3], Colin Franz[3,4,5], Sumanas Jordan[1]

[1]Division of Plastic and Reconstructive Surgery, Department of Surgery, Simpson Querrey Institute, Northwestern University, Chicago, IL 60611, USA, [2]Department of Biomedical Engineering and Simpson Querrey Institute, Northwestern University, Evanston, Illinois 60208, USA, [3]Regenerative Neurorehabilitation Laboratory, Shirley Ryan AbilityLab, Chicago, IL 60611, USA. [4]Department of Physical Medicine and Rehabilitation, Feinberg School of Medicine, Northwestern University, Chicago, IL 60611, USA. [5]The Ken&Ruth Davee Department of Neurology, Feinberg School of Medicine, Northwestern University, Chicago, IL 60611, USA.

Recovering from Volumetric Muscle Loss

Large scale injuries from high-energy impact events are characterized by volumetric muscle loss (VML) and are irreparable by the innate skeletal muscle repair system. This loss of muscle mass exacerbates a reduction in peripheral nerve functionality as a severe consequence of VML. The application of 3D additive manufacturing processes in tissue engineering provides an opportunity to develop patient-specific implants for VML with personalized physical and biochemical properties. Graphene as a biomaterial has gained popularity in the field of rehabilitation due to its highly conductive nature and suitable biocompatibility, properties ideal for the regeneration of excitable tissues. Graphene has also demonstrated an ability to be incorporated into 3D manufacturing solutions, an attribute stemming from its superior mechanical flexibility. A significant drawback of these products, however, is low bioactivity.

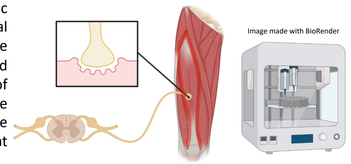

Extracellular matrix (ECM) derived from decellularized tissue offers an approach to mitigate this shortcoming. For VML specifically, decellularized muscle ECM (dECM) contains muscle-specific proteins and growth factors beneficial to tissue regeneration.

Research Objectives

Determine scaffold influence on viability, adhesion, alignment, proliferation, and differentiation of myoblast cell lines.

Characterize viability, adhesion, neurite outgrowth length, and neuronal interconnectivity of induced pluripotent stem cell (iPSC) derived motor neurons on both scaffold variants.

Composition of Graphene-Based Scaffolds

3D composites with and without mouse-pup dECM were fabricated using bioink made primarily of graphene and the biocompatible elastomer, poly(lactide-co-glycolide) (PLGA). Muscle collected from mice pups was put through a series of detergent washes and then lyophilized to collect dECM.

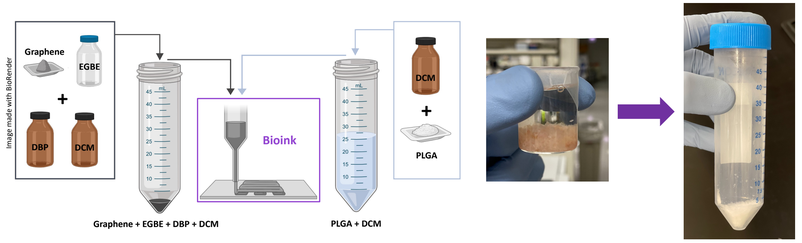

Using an extrusion-based system, graphene structures with and without dECM were printed in four-layered stacks with strut sizes ranging between 125 – 250 µm in width.

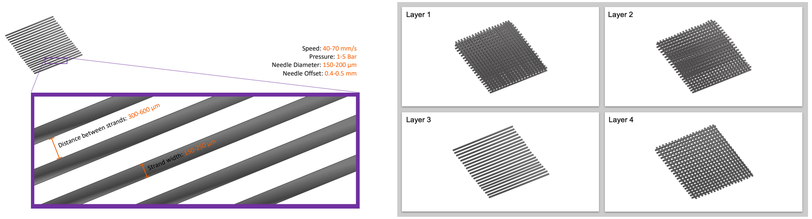

3D Printed Graphene Scaffolds with dECM

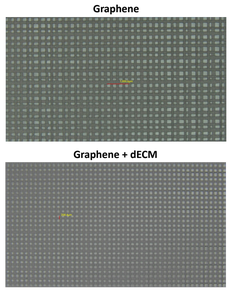

Figure 1: Brightfield images of 3D printed graphene scaffold (top) and graphene scaffold containing 2.5% dECM from mouse pup muscle (bottom).

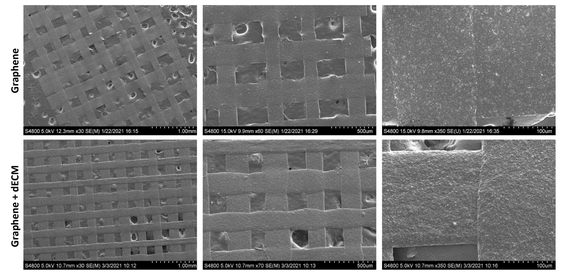

Figure 2: SEM images of 3D printed graphene scaffold (top) and graphene scaffold containing 2.5% dECM from mouse pup muscle (bottom).

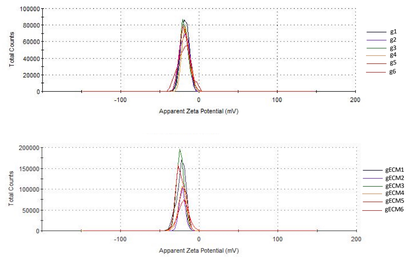

Figure 3: Current/Voltage graphs of 3D printed graphene scaffold (left) and graphene scaffold containing 2.5% dECM from mouse pup muscle (right) for calculating conductivity.

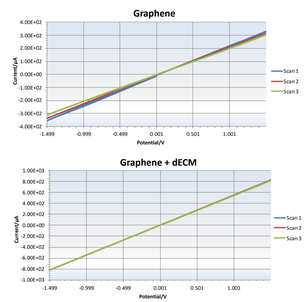

Figure 4: Zeta Potential distribution of 3D printed graphene scaffold (left) and graphene scaffold containing 2.5% dECM from mouse pup muscle (right).

Scaffold Influence on Myoblast Cell Lines

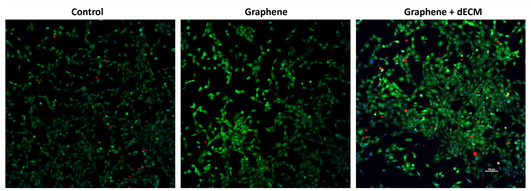

Figure 5: Confocal images showing viability of C2C12 mouse myoblasts after 72 hours on culture plate (left), graphene scaffold (middle), graphene + dECM (2.5%) scaffold (right).

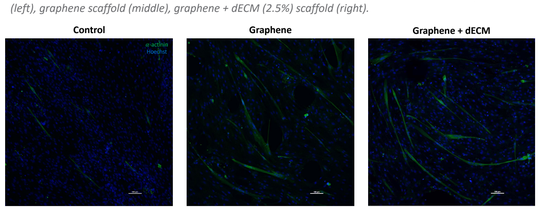

Figure 7: Confocal images showing myotube formation from human myoblasts after 10 days in fusion medium on culture plate (left), graphene scaffold (middle), graphene + dECM (2.5%) scaffold (right).

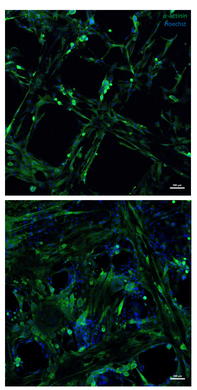

Figure 6: Confocal images of myotube formation from C2C12 mouse myoblasts after 2 weeks in fusion medium: graphene scaffold (top), graphene + dECM (2.5%) scaffold (bottom).

Neurite Outgrowth and Network Formation

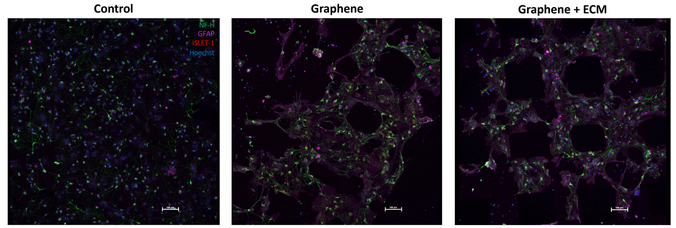

Figure 8: Confocal images showing human iPSC derived motor neurons on glial cells taken from mice in culture dish (left), on graphene scaffold (middle), graphene scaffold containing 2.5% dECM (right).

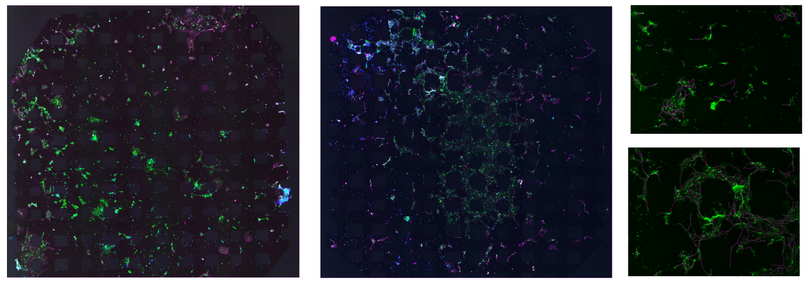

Figure 9: Fluorescent tile-scan images of human iPSC derived motor neurons and glial cells on graphene scaffold (left), graphene scaffold containing 2.5% dECM (middle). Example of neurite counting for graphene scaffold (top right) and graphene scaffold with 2.5% dECM (bottom right). Picture size = 4614 x 4297 microns for macro images, 1245 x 933 microns for zoomed in tiles.

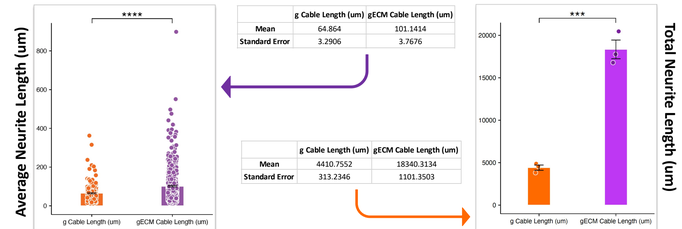

	g Cable Length (um)	gECM Cable Length (um)
Mean	64.864	101.1414
Standard Error	3.2906	3.7676

	g Cable Length (um)	gECM Cable Length (um)
Mean	4410.7552	18340.3134
Standard Error	313.2346	1101.3503

*Figure 10: Average neurite length (left) and total neurite length (right) from motor neurons on graphene (orange) and graphene + dECM (purple) scaffolds. ***p < 0.001, ****p < 0.0001.*

Conclusions

Graphene scaffolds containing 2.5% dECM were found to have a reduced electrical conductivity (74.4 S/m) compared to scaffolds made from graphene alone (286.4 S/m).

Zeta potential values were measured to be -17.9 ± 5.14 mV in graphene scaffolds and -22.7 ± 5.76 mV in gECM scaffolds.

Scanning electron microscopy images showed no distinct differences in surface topography between the two scaffold types.

Graphene and gECM scaffolds both suitable in supporting glial cells and motor neurons; improved neural network interconnectivity observed in motor neurons seeded onto graphene scaffolds containing dECM.

Both scaffold variants effective in supporting C2C12 and human muscle myoblast adhesion, alignment, viability, proliferation, and differentiation. Increased fusion in C2C12 muscle myoblasts were also observed as they differentiated into myotubes on the surface of gECM scaffolds.

Acknowledgements

ECM collection and zeta analysis was performed in the Analytical bioNanoTechnology Core Facility of the Simpson Querrey Institute at Northwestern University. ANTEC is currently supported by the Soft and Hybrid Nanotechnology Experimental (SHyNE) Resource (NSF ECCS-2025633).

Northwestern Medicine® Feinberg School of Medicine

Shirley Ryan AbilityLab